IEEE Access
Multidisciplinary | Rapid Review | Open Access Journal

Received December 7, 2018, accepted January 11, 2019, date of publication January 18, 2019, date of current version February 8, 2019.

Digital Object Identifier 10.1109/ACCESS.2019.2893613

Emitter-Length Scalable Small Signal and Noise Modeling for InP Heterojunction Bipolar Transistors

AO ZHANG, (Student Member, IEEE), AND JIANJUN GAO, (Senior Member, IEEE)
School of Information Science and Technology, East China Normal University, Shanghai 200241, China

Corresponding author: Jianjun Gao (jjgao@ee.ecnu.edu.cn)

This work was supported by the National Natural Science Foundation of China under Grant 61774058.

ABSTRACT In this paper, an emitter-length scalable noise and small signal model for InP heterojunction bipolar transistor (HBT) are presented. A set of scalable expressions for noise parameters based on hybrid-π topology in the low-frequency ranges are derived. The analytical and experimental results show that under the same bias condition, good emitter-length scaling of the noise and small signal model parameters can be achieved between 1.6μm $\times$10 μm, 1.6μm $\times$ 20 μm and 1.6μm $\times$ 30 μm InP HBTs.

INDEX TERMS Equivalent circuits, HBT, semiconductor device modeling, parameter extraction, noise modeling.

I. INTRODUCTION

Accurate noise and small signal circuit model of heterojunction bipolar transistors (HBTs) is very attractive for the prediction of device performance analysis in designing of low noise devices and microwave circuits. Most of monolithic microwave and millimeterwave integrated circuits consist of HBTs with various sizes, the scalable models are essential for designing such circuits.

As well known, the output power from a HBT is dependent on its size, the emitter area is often used to describe the size of HBT's [1]. Therefore, an emitter area scalable noise and small signal model as a function of HBT size is required.

Scaling of the small-signal equivalent circuit model dependent on the sizes of base and emitter regions has been investigated [2]–[6]. Once the scalable normalization rules are obtained, the model parameters of different size devices under the same process condition can be determined. Based on the physical scaling rules of single-cell HBT device, the power performance of multifinger unit cells can be evaluated [7]–[13] and provide feedback for process control data. SiGe HBTs are the first practical bandgap-engineered silicon devices, and the small signal model is complicated due to the influence of the lossy Si well substrate region beneath the collector-bulk junction [14], [15].

A new emitter-length scalable noise model for InP HBT devices based on hybrid π-topology is proposed in this paper. The scalable rules for extrinsic and intrinsic model parameters are developed in detail. The proposed model can be used to predict the S parameters and noise performance of HBTs with different geometry accurately.

This paper is organized as follows. Section II and section III give the scalable equivalent circuit model and corresponding scaling rules. Section IV compares the modeled and measured data with various emitter sizes. The conclusions are discussed in section V.

II. EQUIVALENT CIRCUIT MODEL

Although the hybrid-T model is directly matched to the physics of the device, however, most established large-signal models for HBT devices build upon the Gummel-Poon formulation and reduce to the hybrid-π topology when linearized. Fig.1 shows the HBT small signal and noise circuit model Fig.1 (a) and Fig.1 (b) are the extrinsic and the intrinsic network, respectively.

Based on the relationship between the hybrid-π and T-type model [2]:

$$g_{mo} = \frac{\alpha_o}{R_{be}} \tag{1}$$

$$R_\pi = \frac{R_{be}}{1-\alpha_o} \tag{2}$$

where α_o denotes the intrinsic current gain at low frequency, the common emitter current gain can be expressed from (1) and (2):

$$\beta = \frac{\alpha_o}{1-\alpha_o} = g_{mo}R_\pi \tag{3}$$

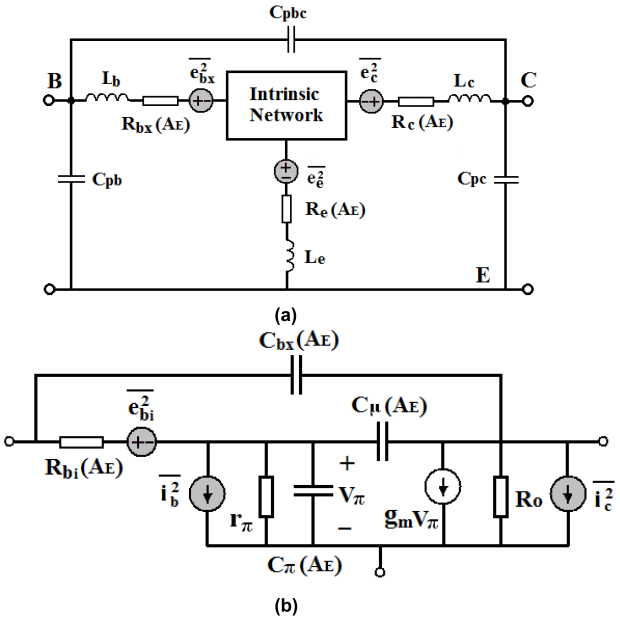

FIGURE 1. Proposed noise and small signal model for HBT. (a) Outer part. (b) Inner part.

The DC current gain β of HBT device is determined by epitaxial growth and processing, the variation of DC current gain β within a wafer is very small and can be neglected, especially the places close to each other. Therefore β can be regard as a parameter which is independent of the device geometry (such as emitter area A_E).

The expression of R_{be} is given as follows:

$$R_{be} = \frac{\eta kT}{qI_E} \approx \frac{\eta kT}{\beta I_B} \tag{4}$$

It can be found that R_{be} is dependent on the base injection current only, and independent of the device geometry.

Based on the discussion above, the transconductance g_m ($g_m = g_{mo}\exp(-j\omega\tau_\pi)$) and input resistance R_π can be regard as the parameters which are independent of the emitter area A_E.

The other small signal model parameters such as the extrinsic and intrinsic base-collector capacitances C_{ex} and C_μ, base-to-emitter capacitance C_π, intrinsic base resistance R_{bi}, and extrinsic resistances are regard as a function of the emitter area A_E.

The two correlated intrinsic current noise sources $\overline{i_b^2}$ and $\overline{i_c^2}$ can be expressed as following [3]–[5]:

$$\overline{i_1^2} = 2qI_B\Delta f \tag{5}$$

$$\overline{i_2^2} = 2qI_C\Delta f \tag{6}$$

$$\overline{i_1^* i_2} = 2qI_C(e^{-j\omega\tau} - 1)\Delta f \tag{7}$$

The noise contributions of the two sources related to the collector current are caused by the same electrons. Therefore, the base current shot noise is correlated to collector current shot noise, and the correlation of these sources is given by a time delay.

It is noted that base and collector currents are independent of the emitter area A_E, therefore the two correlated current noise sources $\overline{i_b^2}$ and $\overline{i_c^2}$ only dependent on the base and collector currents.

III. SCALING OF MODEL PARAMETERS

It is well known, the pad capacitances and feedline inductances do not need any scaling [15], [16]. The scaling rules of other small signal and noise model parameters will developed in the following.

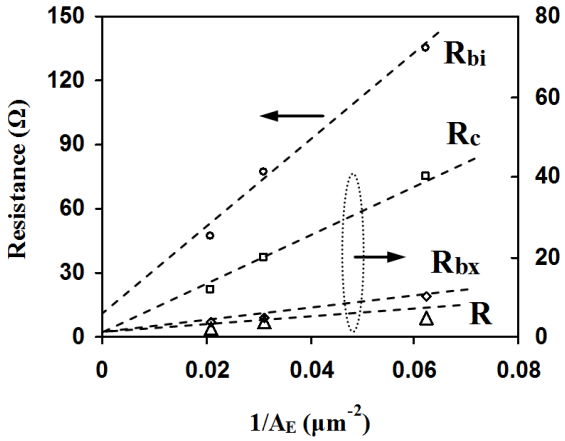

FIGURE 2. Extrinsic resistances versus emitter area.

A. SCALING OF SMALL SIGNAL MODEL PARAMETERS

Fig.2 shows the extracted extrinsic resistances R_{bx}, R_c and R_e versus emitter area A_E, it is clearly that the three extrinsic resistances are inversely proportional to the emitter area. Meanwhile the intrinsic base resistance R_{bi} is a linear function of reciprocal of A_E and can be expressed as following:

$$R_{bi} = R_{bio} + \frac{R_{bi}^u}{A_E} \tag{8}$$

where $R_{bio} = 12\Omega$ and $R_{bi}^u = 2000\Omega \cdot \mu\text{m}^2$

Fig.3(a) shows the extracted capacitances C_π, C_{ex} and C_{bc} versus emitter area A_E, it can be found that the intrinsic capacitances C_π and C_{bc} are proportional to the emitter area. The extrinsic base-collector capacitance C_{ex} is a linear function of A_E, and can be expressed as following:

$$C_{ex} = C_{exo} + C_{ex}^u A_E \tag{9}$$

where $C_{exo} = 13\text{fF}$ and $C_{ex}^u = 0.56\text{fF}/\mu\text{m}^2$

Fig.3 (b) shows the extracted g_{mo}, R_o and R_π versus emitter area A_E, it can be found that all of these parameters are independent of device geometry.

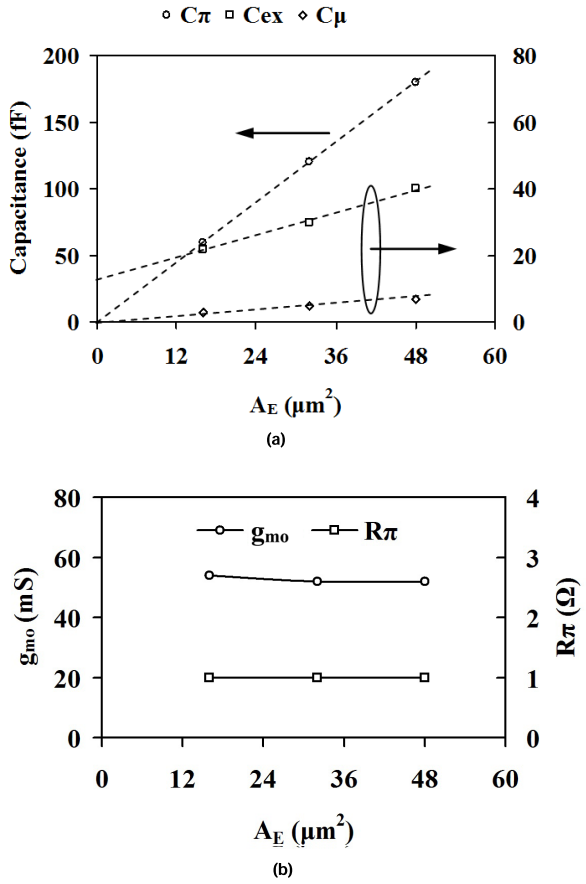

FIGURE 3. Intrinsic elements versus emitter area. (a) C_π, C_{ex} and C_μ. (b) g_{mo}, R_o and R_π.

From Fig.2 ∼3, it is obviously that the scaling formulas are determined to be as follows:

$$\begin{bmatrix} C_\pi \\ C_\mu \\ C_{ex} \\ R_{bi} \\ R_{bx} \\ R_c \\ R_e \end{bmatrix} = \begin{bmatrix} A_E & 0 & 0 & 0 & 0 & 0 & 0 \\ 0 & A_E & 0 & 0 & 0 & 0 & 0 \\ 0 & 0 & A_E & 0 & 0 & 0 & 0 \\ 0 & 0 & 0 & A_E^{-1} & 0 & 0 & 0 \\ 0 & 0 & 0 & 0 & A_E^{-1} & 0 & 0 \\ 0 & 0 & 0 & 0 & 0 & A_E^{-1} & 0 \\ 0 & 0 & 0 & 0 & 0 & 0 & A_E^{-1} \end{bmatrix} \begin{bmatrix} C_\pi^u \\ C_\mu^u \\ C_{ex}^u \\ R_{bi}^u \\ R_{bx}^u \\ R_c^u \\ R_e^u \end{bmatrix} + \begin{bmatrix} 0 \\ 0 \\ C_{exo} \\ R_{bio} \\ 0 \\ 0 \\ 0 \end{bmatrix} \tag{10}$$

where u denotes the unit area.

B. SCALING OF NOISE MODEL PARAMETERS

Based on the noise correlation matrix technique [17], [18], the noise model parameter can be carried out as shown in Table 1.

It can be found that all the noise model parameters I_b, I_c and time delay τ are remain invariant approximately. Noted that

TABLE 1. Extracted noise model parameter.

Parameters	1.6μm × 10μm	1.6μm × 20μm	1.6μm × 30μm
I_b (μA)	40	40	40
I_c (mA)	2.06	2.0	2.04
τ (pS)	0.5	0.5	0.5

minimum noise figure $F_{\min}$, noise resistance R_n, optimum source conductance G_{opt} and optimum source susceptance B_{opt} can be determined directly from these three noise model parameters.

In the lower frequency ranges (normally less than 5GHz), the influence of the extrinsic inductances can be neglected, and the correlation between the noise sources is zero. Based on the noise correlation matrix calculation method [17] [18], the intrinsic part noise matrix can be calculated. After adding the influence the extrinsic elements, the four noise parameters can be expressed as following:

$$R_n = aA_E^{-2} + bA_E^{-1} + c \tag{11}$$

$$B_{opt} = d + eA_E \tag{12}$$

$$G_{opt} = \sqrt{\frac{f}{aA_E^{-2} + bA_E^{-1} + c}} \tag{13}$$

$$F_{\min} = g + mA_E^{-1} + n\sqrt{aA_E^{-2} + bA_E^{-1} + c} \tag{14}$$

where

$$\begin{aligned} a &= (R_{bi}^u)^2 \\ b &= 2R_{bi}^u(\frac{1}{g_m} + R_{bi}^u) + R_{bi}^u + R_{bx}^u + R_e^u \\ c &= \frac{I_C}{2V_T g_m^2} + (\frac{1}{g_m} + R_{bi}^u)^2 + R_{bio} \\ d &= -\omega(C_{pg} + C_{exo}) \\ e &= -\omega[C_{ex}^u + C_{bc}^u + \frac{C_\pi^u}{(1 + g_m R_{bi})^2}] \\ f &= \frac{I_B}{2V_T} \\ g &= 1 + 2fR_{bio} \\ m &= 2fR_{bi}^u \\ n &= 2\sqrt{\frac{I_B}{2V_T}} \end{aligned}$$

From (11)-(14), it is obviously that the noise resistance R_n can be expressed as a quadratic function of reciprocal of A_E because the intrinsic and extrinsic resistances decrease with the increase of the device emitter area A_E. The optimum source conductance G_{opt} is inversely proportional to the noise resistance R_n, and increases with increase of the device emitter area A_E. The optimum source susceptance B_{opt} is determined mainly by base-collector and base-emitter junction capacitances. It is noted that when $g_m R_{bi} >> 1$, the effect of C_π on B_{opt} can be neglected, therefore B_{opt} can be regard as a linear function of device emitter area A_E. The minimum noise figure $F_{\min}$ is a linear function of the

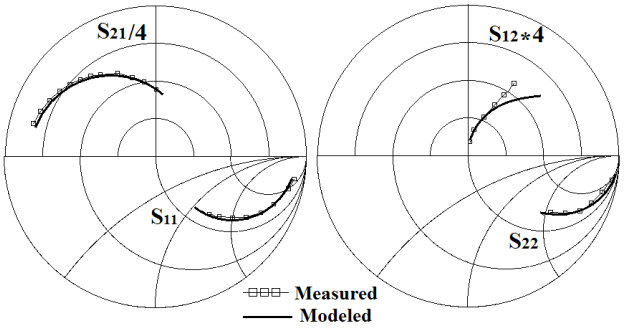

FIGURE 4. Comparison of modeled and measured S parameters for the 1.6μm × 10μm HBT. Bias: $I_b = 40\mu$A, $V_{ce} = 1.5$V.

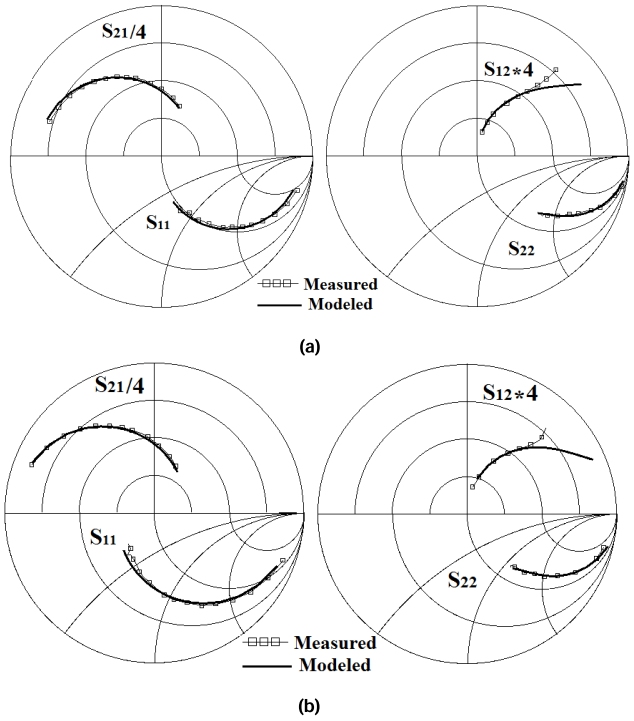

FIGURE 5. Comparison of S parameters between measured and scaled HBT devices. Bias: $I_b = 40\mu$A, $V_{ce} = 1.5$V. (a) 1.6μm × 20μm HBT. (b) 1.6μm × 30μm HBT.

noise resistance R_n and reciprocal of A_E, of course decreases with increase of the device emitter area.

IV. EXPERIMENTAL VERIFICATION

In order to verify the above results, a set of noise and small signal model parameters are determined for InP/InGaAs DHBTs with different emitter area 1.6μm × 10μm, 1.6μm × 20μm and 1.6μm × 30μm. Details of the device structure and fabrication technique have been described elsewhere [19]. Microwave noise parameter measurements are carried out on wafer over the frequency range 2-20GHz using an ATN microwave noise measurement system NP5.

A. SMALL SIGNAL MODEL VERIFICATION

Fig.4 compares the measured and modeled S parameters for the 1.6μm × 10μm HBT in the frequency range of 2GHz to 20GHz under $I_b = 40\mu$A, $V_{ce} = 1.5$V bias condition. Fig.5 shows good agreement in S-parameters between

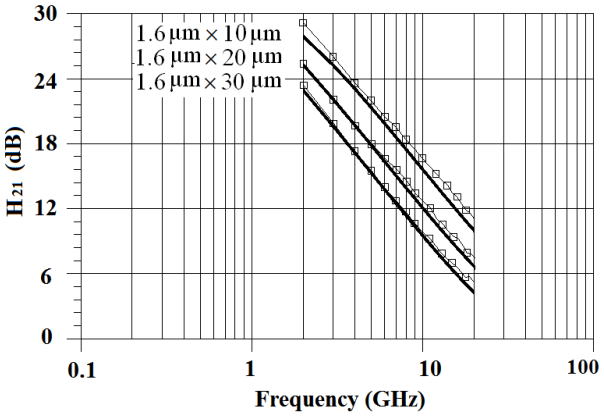

FIGURE 6. Comparison of modeled and measured short circuit gain for HBT devices with different emitter area (after de-embedding the pad capacitances).

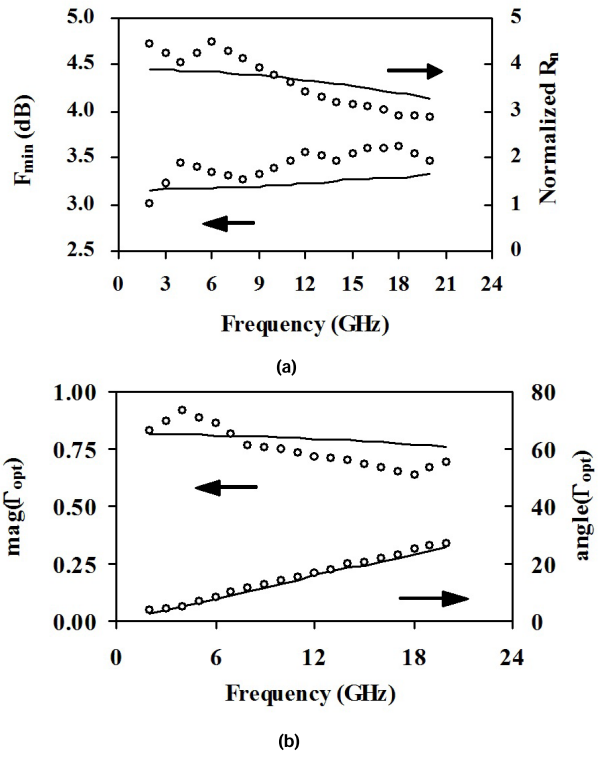

FIGURE 7. Comparison of measured and modeled noise parameters for the 1.6μm × 10 μm HBT. Bias: $I_b = 40\mu$A, $V_{ce} = 1.5$V.

the measured and the scaled models determined by using the scaling rules for 1.6μm × 20μm and 1.6μm × 30μm HBT devices. The short circuit gain comparison between modeled and measured data for HBT devices with different emitter area is shown in Fig.6. The corresponding cut-off frequencies f_t are 80GHz, 50GHz and 35GHz roughly under same bias conditions (after de-embedding the pad capacitances).

B. NOISE MODEL VERIFICATION

Fig.7 shows the comparison of measured and modeled noise parameters for the 1.6μm × 10μm HBT under bias condition

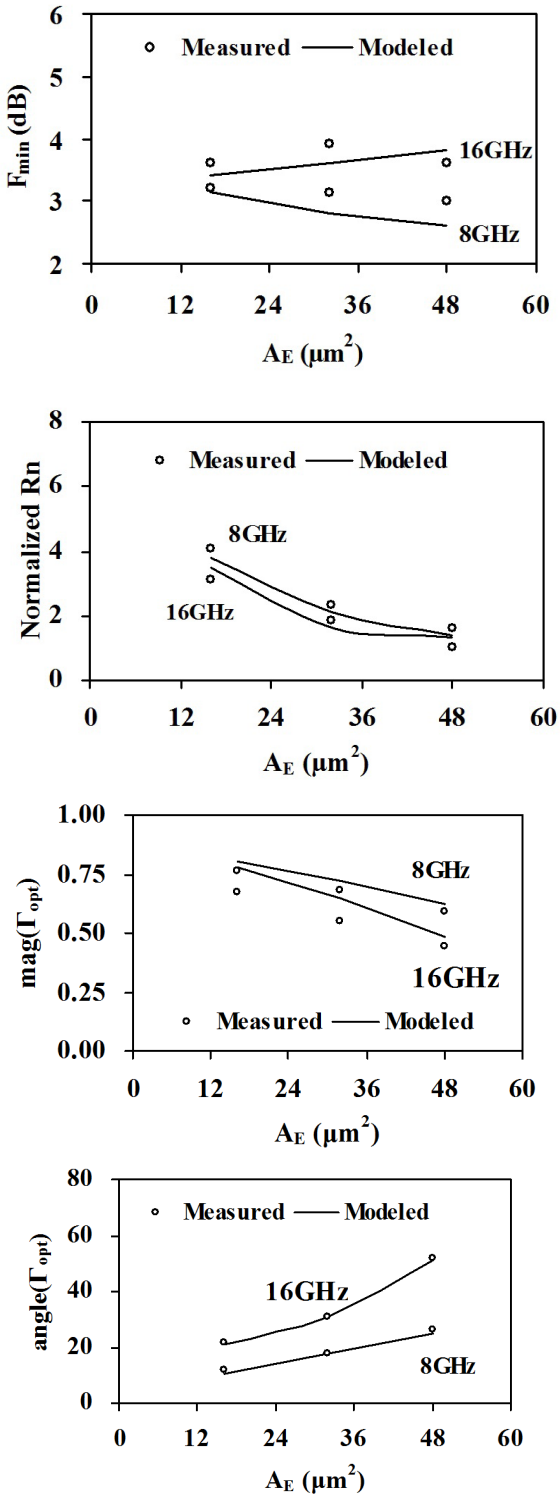

FIGURE 8. Comparison of measured and modeled noise parameters as a function of emitter area at 8GHz and 16GHz. Bias: $I_b = 40\mu A$, $V_{ce} = 1.5V$.

$I_b = 40\mu A$ and $V_{ce} = 1.5V$. Good agreement over the whole frequency range 2-20GHz is obtained. Fig.8 shows the comparison of measured and modeled noise parameters as a function of emitter area by using the scaling rules at two different frequency points.

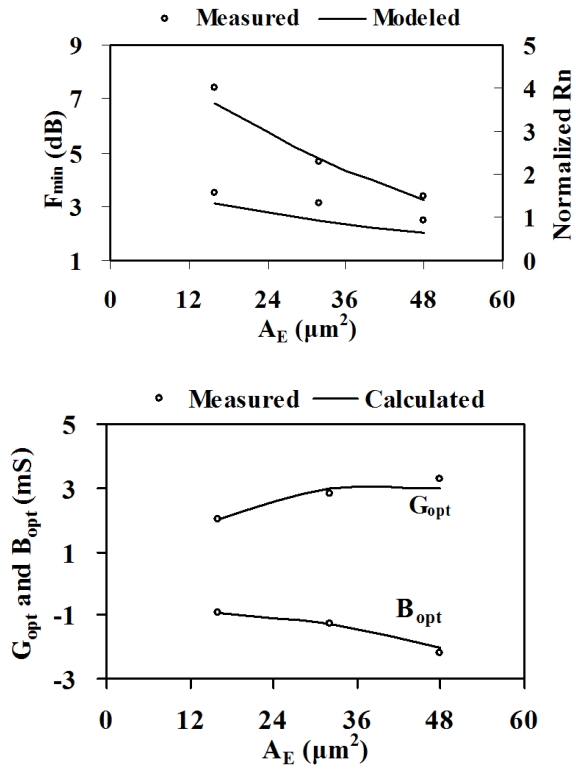

FIGURE 9. Comparison between measured and calculated noise parameters as a function of emitter area at 4GHz. Bias: $I_b = 40\mu A$, $V_{ce} = 1.5V$.

Fig.9 shows the calculated noise parameters (from Eq.(11)-(14)) and measured data versus frequency for the InP HBT under the same bias conditions ($I_b = 40\mu A$, $V_{ce} = 1.5V$). Good agreement is observed. It can be found that minimum noise figure $F_{\min}$ decreases slowly with the increase of the emitter area, and the noise resistance R_n decreases rapidly with increasing the emitter area. The optimum source susceptance B_{opt} increases with increase of the device emitter area, and is a linear function approximately.

V. CONCLUSION

The relationship between noise model parameters and emitter-length for HBT is developed in this paper. A set of analytical expressions of noise parameters are given, and experimental results show that under same bias condition, good scaling of the noise and small signal model parameters can be achieved between $1.6\mu m \times 10\mu m$, $1.6\mu m \times 20\mu m$ and $1.6\mu m \times 30\mu m$ InP HBTs.

REFERENCES

[1] F. Ali, *HEMTs and HBTs: Devices, Fabrication, and Circuits*. Norwood, MA, USA: Artech House, 1991, pp. 311–315.
[2] J. Gao, *Heterojunction Bipolar Transistors for Circuit Design: Microwave Modeling and Parameter Extraction*. Singapore: Wiley, 2015.
[3] M. Rudolph, R. Doerner, E. Richter, and P. Heymann, "Scaling of GaInP/GaAs HBT equivalent-circuit elements," in *GAAS Dig.*, 1999, pp. 113–116.
[4] D.-W. Wu, M. Fukuda, Y.-H. Yun, and D. L. Miller, "Small-signal equivalent circuit scaling properties of AlGaAs/GaAs HBTs," in *IEEE MTT-S Int. Microw. Symp. Dig.*, Orlando, FL, USA, May 1995, pp. 631–634.

[5] M. J. W. Rodwell *et al.*, "Submicron scaling of HBTs," *IEEE Trans. Electron Devices*, vol. 48, no. 11, pp. 2606–2624, Nov. 2001.
[6] S.-C. Huang, W.-B. Tang, and Y.-M. Hsin, "High-frequency noise modeling of InGaP/GaAs HBT with base-contact capacitance and AC current crowding effect," *IEEE Electron Device Lett.*, vol. 30, no. 11, pp. 1125–1127, Nov. 2009.
[7] T. Nardmann, P. Sakalas, F. Chen, T. Rosenbaum, and M. Schroter, "A geometry scalable approach to InP HBT compact modeling for mm-Wave applications," in *Proc. IEEE Compound Semiconductor Integr. Circuit Symp.*, Oct. 2013, pp. 1–4.
[8] T. Nardmann, M. Schröter, P. Sakalas, and B. Lee, "A length-scalable compact model for InP DHBTs," in *Proc. IEEE Semiconductor Conf. Dresden-Grenoble*, Sep. 2013, pp. 1–4.
[9] H.-C. Wu, S. Mijalkovic, and J. N. Burghartz, "A referenced geometry based configuration scalable Mextram model for bipolar transistors," in *Proc. IEEE Int. Behav. Modeling Simulation Workshop*, Sep. 2006, pp. 50–55.
[10] C. Raya, F. Pourchon, T. Zimmer, D. Céli, and P. Chevalier, "Scalable approach for HBT's base resistance calculation," *IEEE Trans. Semicond. Manuf.*, vol. 21, no. 2, pp. 186–194, May 2008.
[11] R. Hajji, F. M. Ghannouchi, and A. B. Kouki, "A systematic layout-based method for the modeling of high-power HBT's using the scaling approach," *IEEE Trans. Electron Devices*, vol. 42, no. 3, pp. 528–533, Mar. 1995.
[12] M. Rudolph, R. Doerner, K. Beilenhoff, and P. Heymann, "Scalable GaInP/GaAs HBT large-signal model," *IEEE Trans. Microw. Theory Techn.*, vol. 48, no. 12, pp. 2370–2376, Dec. 2000.
[13] U. Schaper and P. Zwicknagl, "Physical scaling rules for AlGaAs/GaAs power HBTs based on a small-signal equivalent circuit," *IEEE Trans. Microw. Theory Techn.*, vol. 46, no. 7, pp. 1006–1009, Jul. 1998.
[14] P. Sakalas and M. Schroter, "Microwave noise in InP and SiGe HBTs: Modeling and challenges," in *Proc. 22nd Int. Conf. Noise Fluctuations (ICNF)*, Jun. 2013, pp. 1–6.
[15] J.-S. Rieh, D. Greenberg, A. Stricker, and G. Freeman, "Scaling of SiGe heterojunction bipolar transistors," *Proc. IEEE*, vol. 93, no. 9, pp. 1522–1538, Sep. 2005.
[16] J. Gao, X. Li, H. Wang, and G. Boeck, "Improved analytical method for determination of small-signal equivalent-circuit model parameters for InP/InGaAs HBTs," *IEE Proc.-Circuits Devices Syst.*, vol. 152, no. 6, pp. 661–666, Dec. 2005.
[17] H. Hillbrand and P. Russer, "An efficient method for computer aided noise analysis of linear amplifier networks," *IEEE Trans. Circuits Syst.*, vol. CAS-23, no. 4, pp. 235–238, Apr. 1976.
[18] J. Gao, X. Li, H. Wang, and G. Boeck, "Microwave noise modeling for InP-InGaAs HBTs," *IEEE Trans. Microw. Theory Tech.*, vol. 52, no. 4, pp. 1264–1272, Apr. 2004.
[19] H. Wang *et al.*, "Demonstration of aluminum-free metamorphic InP/In0.53Ga0.47As/InP double heterojunction bipolar transistors on GaAs substrates," *IEEE Electron Device Lett.*, vol. 21, no. 9, pp. 427–429, Oct. 2000.

AO ZHANG was born in Nanjing, Jiangsu, China, in 1995. She received the B.S. degree in electrical engineering from the Nanjing University of Posts and Telecommunications, Nanjing, in 2017. She is currently pursuing the Ph.D. degree with East China Normal University, Shanghai, China.

Her research interests include modeling and on-wafer millimeter-wave measurements of active and passive devices.

JIANJUN GAO was born in Hebei, China, in 1968. He received the B.Eng. and Ph.D. degrees from Tsinghua University, Beijing, China, in 1991 and 1999, respectively, and the M.Eng. degree from the Hebei Semiconductor Research Institute, Hebei, in 1994. From 1999 to 2001, he was a Postdoctoral Research Fellow at the Microelectronics Research and Development Center, Chinese Academy of Sciences, Beijing, where he was developing the PHEMT optical modulator driver. In 2001, he joined the School of Electrical and Electronic Engineering, Nanyang Technological University, Singapore, as a Research Fellow in semiconductor device modeling and on wafer measurement. In 2003, he joined the Institute for High-Frequency and Semiconductor System Technologies, Berlin University of Technology, Berlin, Germany, as a Research Associate, where he was involved in the InP HBT modeling and circuit design for high speed optical communication. In 2004, he joined Electronics Engineering Department, Carleton University, Ottawa, ON, Canada, as Postdoctoral Fellow, where he was involved in the semiconductor neural network modeling technique. From 2004 to 2007, he was a Full Professor with the Radio Engineering Department, Southeast University, Nanjing, China. Since 2007, he has been a Full Professor with the School of Information Science and Technology, East China Normal University, Shanghai, China. He has authored *RF and Microwave Modeling and Measurement Techniques for Field Effect Transistors* (USA: SciTech Publishing, 2009) and *Optoelectronic Integrated Circuit Design and Device Modeling* (New York: Wiley, 2010). His research interests include characterization, modeling, and on wafer measurement of microwave semiconductor devices, optoelectronics device and high-speed integrated circuit for radio frequency, and optical communication.